Future decreases in thermospheric density in very low Earth orbit

Matthew Kenneth Brown[1], Hugh Lewis[1], Andrew John Kavanagh[2], and Ingrid Cnossen[2]

[1]University of Southampton
[2]British Antarctic Survey

November 23, 2022

Abstract

Increasing carbon dioxide causes cooling in the upper atmosphere and a secular decrease in atmospheric density over time. With the use of the Whole Atmospheric Community Climate Model with thermosphere and ionosphere extension (WACCM-X), neutral thermospheric densities up to 500 km have been modelled under increasing carbon dioxide concentrations. Only carbon dioxide and carbon monoxide concentrations are changed between simulations, and solar activity is held low at F10.7 = 70 throughout. Using the four Representative Concentration Pathway (RCP) carbon dioxide scenarios produced by the Intergovernmental Panel on Climate Change (IPCC), scenarios of neutral density decrease through to the year 2100 have been modelled. The years 1975 and 2005 have also been simulated, which indicated a historic trend of -5.8% change in neutral density per decade. Decreases in the neutral density relative to the year 2000 have been given for increasing ground-level carbon dioxide concentrations. WACCM-X shows there has already been a 17% decrease in neutral densities at 400 km relative to the density in the year 2000. This becomes a 30% reduction at the 50:50 probability threshold of limiting warming to 1.5 degrees Celsius, as set out in the Paris Agreement. A simple orbital propagator has been used to show the impact the decrease in density has on the orbital lifetime of objects travelling through the thermosphere. If the 1.5 degrees Celsius target is met, objects in LEO will have orbital lifetimes around 30% longer than comparable objects from the year 2000.

Future decreases in thermospheric density in very low Earth orbit

M. K. Brown[1], H. G. Lewis[1], A. J. Kavanagh[2], I. Cnossen[2]

[1]University of Southampton, Aeronautical and Astronautical Engineering, Faculty of Engineering and Physical Sciences, Boldrewood Innovation Campus, Southampton, SO16 7QF, United Kingdom
[2]British Antarctic Survey, High Cross, Madingley Road, Cambridge, CB3 0ET, United Kingdom

Key Points:

- The reduction in future thermospheric densities at low Earth orbit altitudes due to increasing carbon dioxide has been simulated.
- Meeting the 1.5 degrees Paris agreement target limits the reduction in density at 400 km altitude since the year 2000 to around 28 percent.
- Objects in LEO will have orbital lifetimes around 30 percent larger at the 1.5 degree target than comparable objects from the year 2000.

Corresponding author: Matthew K. Brown, `mkb1g12@soton.ac.uk`

Abstract

Increasing carbon dioxide causes cooling in the upper atmosphere and a secular decrease in atmospheric density over time. With the use of the Whole Atmospheric Community Climate Model with thermosphere and ionosphere extension (WACCM-X), neutral thermospheric densities up to 500 km have been modelled under increasing carbon dioxide concentrations. Only carbon dioxide and carbon monoxide concentrations are changed between simulations, and solar activity is held low at $F_{10.7} = 70$ throughout. Using the four Representative Concentration Pathway (RCP) carbon dioxide scenarios produced by the Intergovernmental Panel on Climate Change (IPCC), scenarios of neutral density decrease through to the year 2100 have been modelled. The years 1975 and 2005 have also been simulated, which indicated a historic trend of -5.8% change in neutral density per decade. Decreases in the neutral density relative to the year 2000 have been given for increasing ground-level carbon dioxide concentrations. WACCM-X shows there has already been a 17% decrease in neutral densities at 400 km relative to the density in the year 2000. This becomes a 30% reduction at the 50:50 probability threshold of limiting warming to 1.5°C, as set out in the Paris Agreement. A simple orbital propagator has been used to show the impact the decrease in density has on the orbital lifetime of objects travelling through the thermosphere. If the 1.5°C target is met, objects in LEO will have orbital lifetimes around 30% longer than comparable objects from the year 2000.

Plain Language Summary

The atmosphere extends upwards into the lower regions of space. Here, carbon dioxide causes cooling of the atmosphere and a decrease in atmospheric density. These density reductions have been simulated for increasing CO_2 concentrations up to an altitude of 500 km by computationally modelling the Earth's atmosphere. For reference, the International Space Station orbits at around 400 km. Density reductions up to the year 2100 have been given for the four CO_2 concentration scenarios published by the Intergovernmental Panel on Climate Change (IPCC). The model has shown there has already been a 17% decrease in atmospheric density at an altitude of 400 km since the year 2000. This will reach a maximum of 30% if the Paris Agreement target to limit global warming to 1.5°C is met. Objects in low Earth orbit travel through the thin, upper atmosphere. A reduction in density at these altitudes means a decrease in the already small amount of atmospheric drag that orbiting objects experience. This increases the amount of time it takes for them to fall out of orbit. If the 1.5°C target is met, orbital lifetimes will be 30% longer than those in the year 2000.

1 Introduction

While there is global warming in the lower atmosphere, the opposite is true in the upper atmosphere where carbon dioxide (CO_2) contributes to global cooling (Roble & Dickinson, 1989). CO_2 molecules gain energy by collisional excitation, notably with atomic oxygen (O), or by absorption of infrared (IR) radiation (Sharma & Roble, 2002). Energy can also be lost from excited CO_2 via collisions with other atmospheric molecules or via IR radiation emission at a wavelength of 15 μm. In the lower atmosphere this IR radiation is quickly reabsorbed leading to warming, but in the much thinner upper atmosphere, the radiation is lost to space or the lower atmosphere and leads to cooling. In the thermosphere, this cooling results in thermospheric contraction and a secular decrease in neutral density at any given altitude in the upper atmosphere (Laštovička et al., 2006). Solar activity also affects thermospheric densities, with the solar cycle causing an oscillatory variation in densities of an order of magnitude (Hathaway, 2015).

The secular decrease in thermospheric density caused by an increase in CO_2 concentration is of particular concern for all objects orbiting in the Low Earth Orbit (LEO) region. With decreasing atmospheric density, an orbiting object experiences less atmo-

Table 1. Observations and models of the historic density trend at 400 km and for low solar activities only.

	Type	$F_{10.7}$ (sfu)	Period	Density trend (% per decade)
Keating et al., 2000	Observation	∼75	1976, 1986 & 1996	-5.04 ± 1.4%
Qian et al., 2006	Model	70	1970-2000	-2.5%
Emmert et al., 2008	Observation	<75	1967-2007	-5.5 ± 1.4%
Saunders et al., 2011	Observation	<90	1970-2010	-7.2%
Emmert, 2015	Observation	60 to 75	1967-2005	-3.1 ± 1.6% [a]
Emmert, 2015	Observation	60 to 75	1967-2013	-7.2 ± 1.2% [a]
Solomon et al., 2015	Model	70	1996-2008	-4.9% (-6.8% at higher k_q)[b]
Solomon et al., 2018	Model	70	1974-2003	-3.9%
This study	Model	70	1975-2005	-5.8%

[a] The trend in Emmert (2015) changes depending on the period it is calculated over
[b] k_q, CO_2-O collisional deactivation rate, of $\sim 1.5 \times 10^{-12}\text{cm}^3\text{s}^{-1}$ and $3.0 \times 10^{-12}\text{cm}^3\text{s}^{-1}$

spheric drag. This becomes particularly relevant at altitudes below 500 km where drag is a dominant perturbing force and the effect of a secular density trend is substantial. The smaller drag force leads to a reduced rate of semi-major axis decrease, and hence a longer orbital lifetime. Observations of changes in the semi-major axis of LEO objects have historically been used to measure density trends (Keating et al., 2000; Emmert et al., 2008; Saunders et al., 2011; Emmert, 2015). Numerical atmospheric models have also been used to simulate historical time periods and estimate the magnitude of density trends associated with an increase in CO_2 concentration (Qian et al., 2006; Solomon et al., 2015, 2018). Results from both groups of studies, at an altitude of 400 km, and found under low solar activities are summarized in Table 1. All of these studies have found the historical secular trend to be negative, with values ranging from -2.5% to -7.2% per decade. The magnitude of the trend is inversely proportional to the level of solar activity (Emmert, 2015; Solomon et al., 2019), so the largest secular changes in neutral density are seen during low solar activity.

Space debris in LEO also have their orbital lifetimes increased due to the declining thermospheric density. Made up of all the discarded components and collision fragments left over from human activity in orbit, space debris poses a substantial risk to operational spacecraft (ESA Space Debris Office, 2020). The number of trackable objects (greater than 10 cm in size) intersecting the LEO region continues to increase, reaching nearly 17,500 in 2020, of which around 2300 are active spacecraft. As the amount of debris increases, so does the probability of a collision which would create further debris. This poses further risk to active spacecraft and disruption to operations as spacecraft operators have to respond to possible conjunctions.

Space debris models have been created to investigate the evolution of the debris environment. However, the decreasing thermospheric density trend has not been included in the majority of these models. Simulations can run many decades, even centuries into the future, over which secular density trends will have an important cumulative effect. The models are also used to assess possible ways to reduce the amount of debris and the risk it poses. One method for operators to reduce the risk posed by space debris in the future is to follow the voluntary debris mitigation guidelines introduced by the United Nation's Committee on the Peaceful Use of Outer Space (UN COPUOS), which includes the limiting of orbital lifetime to 25 years once a satellite's mission is complete. Another method known as Active Debris Removal (ADR) is the launching of satellites with the

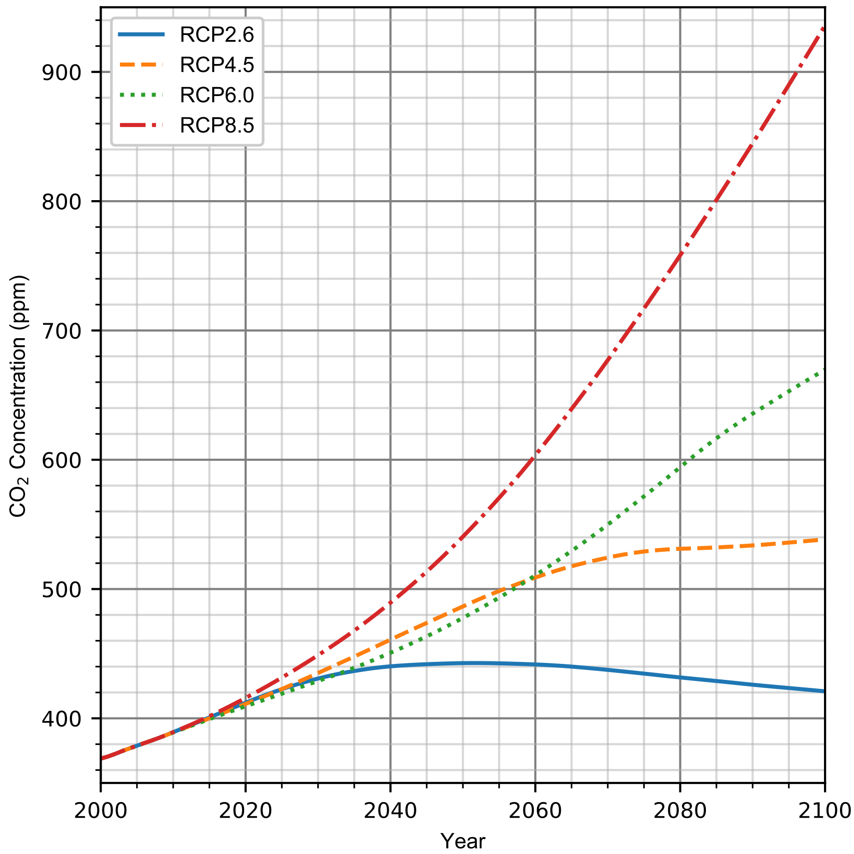

Figure 1. Four ground-level carbon dioxide trajectories through to the year 2100 (RCP Database, 2009). These were released by the IPCC in its fifth assessment report in 2014 (IPCC, 2014). Concentrations previous to 2014 are measured global averages.

aim of removing the pieces of space debris which pose the greatest risk to the environment.

The Intergovernmental Panel on Climate Change (IPCC)'s Fifth Assessment Report (AR5) published four Representative Concentration Pathways (RCPs), with each giving a CO_2 trajectory through to the year 2100. These are shown in Figure 1 and summarized in the Synthesis Report from the IPCC (2014). These are entitled RCP2.6, RCP4.5, RCP6.0 and RCP8.5, where the number refers to the radiative forcing in W/m^2 in the year 2100 for each scenario. While these are not meant to be predictions of the future, they provide a limited number of baseline scenarios and CO_2 concentration trajectories from which modelling can be performed and results across studies compared. The RCPs are used to predict future density reductions and trends within this work.

2 Model simulations

The Community Earth System Model (CESM) from the National Center for Atmospheric Research (NCAR) allows for simulation of the whole, coupled Earth climate, using separate modules for each major system. In this work, the Whole Atmosphere Community Climate Model - eXtended (WACCM-X) module is used (Liu et al., 2010). This

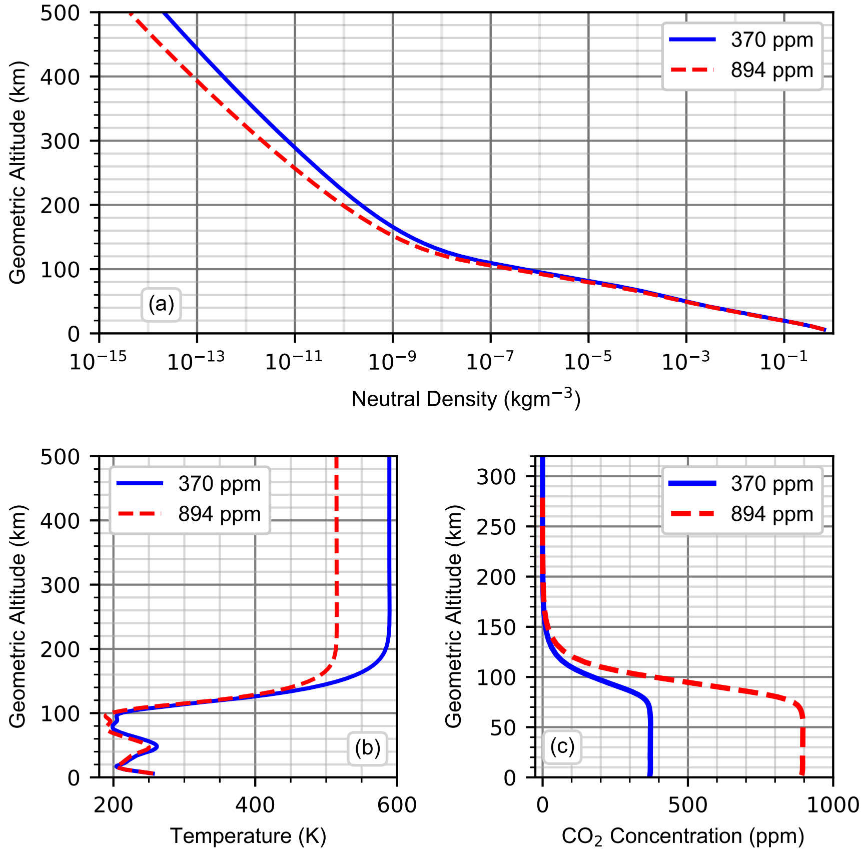

Figure 2. Blue solid lines relate to the year 2000 with a ground-level CO_2 concentration of 370 ppm. Red dashed lines relate to the year 2095 under the RCP8.5 scenario at 894 ppm, the highest CO_2 concentration modelled. The plots show global mean annual means where (a) is the neutral density profile, (b) the temperature profile and (c) the CO_2 concentration profile.

models the atmosphere numerically from ground level through to 4×10^{-10} hPa, which corresponds to an altitude of 350 km at CO_2 levels from the year 2000 and low solar activity. The model has a resolution of 1.9° in latitude and 2.5° in longitude (using a 96 by 144 grid), with 81 vertical pressure levels and a resolution of one-quarter scale height above 1 hPa. Solar and geomagnetic activity are parametrized in the model using established indices of activity such as the solar 10.7 cm radio flux, $F_{10.7}$, and the planetary Kp index respectively. For a full description of the model, including the chemistry and radiative transfer within WACCM-X, see Liu et al. (2010). For this work, CESM 1.2.2 was run on the University of Southampton computing cluster, Iridis 4.

There are only small variations in carbon dioxide concentration from ground level up to around 70 km where the atmosphere is well mixed. Above this altitude molecular diffusion takes over and the concentration reduces towards 0 ppm, as seen in Figure 2c. New initial conditions for WACCM-X under varying CO_2 concentrations were created by scaling the CO_2 values at each pressure level in the original files (here chosen as the WACCM-X default files for the year 2000) by the relative increase in ground-level CO_2 concentration. At the higher altitudes, CO_2 and carbon monoxide (CO) exist in chemical equilibrium. To account for this, CO values are scaled similarly to CO_2. This accounts for over 99.7% of the carbon in the thermosphere and minor constituents containing carbon such as methane (CH_4) were not scaled. However, the effect of changes in methane on thermospheric density is expected to be much smaller than the effect of the increase in CO_2 concentration (Roble & Dickinson, 1989).

Nitric oxide (NO) also plays an important role in thermospheric cooling during solar maximum (Mlynczak et al., 2016), and could be increased by the anthropogenic emission of the greenhouse gas nitrous oxide (N_2O). However, the large amount of Nitrogen (N_2) in the lower atmosphere acts as a reservoir, keeping NO in the thermosphere at a relatively stable level. To remove the effects of solar activity (and therefore also NO) on cooling and the secular density trend, the $F_{10.7}$ and Kp indices were held fixed at 70 sfu and 0.33 respectively in all simulations.

The Earth's magnetic field also changes over time, affecting the ionosphere and in turn the thermosphere (Cnossen, 2014). It was found that for the period 1908 to 2008, the historic changes in the magnetic field do contribute to cooling at 300 km, however, the increasing CO_2 concentration dominates the thermospheric cooling. A recent study by Cnossen and Maute (2020) confirmed the predicted changes in the Earth's magnetic field up to the year 2065 will result in at most a 1-2% increase in density from 2015 to 2065, and so will not be important for future trends in thermosphere density. The impact of the changing magnetic field will therefore not be considered in this paper. The magnetic field within WACCM-X, namely the International Geomagnetic Reference Field (IGRF-12) described in Thébault et al. (2015), is held fixed at the year 2000 level.

The CO_2-O collisional deactivation rate (quenching rate), k_q, has a major impact on the cooling within atmospheric models, as can be seen by the change in density trend of Solomon et al. (2015) from -4.9% per decade at $k_q = \sim 1.5\times10^{-12}$ cm^{3}s^{-1} to -6.8% at $k_q = 3.0 \times 10^{-12}$ cm^{3}s^{-1}. Recent measurements of the value vary between 1.5×10^{-12} and 8.0×10^{-12} cm^{3}s^{-1} and are summarised in Feofilov et al. (2012). The value of k_q used for this study has been left as the default in WACCM-X, namely 3.0×10^{-12} cm^{3}s^{-1} as this was the value WACCM-X was calibrated with during development.

WACCM-X performed simulations of 10 different ground-level CO_2 concentrations, each for 16 model months total. These are the CO_2 concentrations of RCP8.5 at 10 year intervals starting from 2005 and ending on 2095, along with the year 1975 (for validation against previous studies). Numerical models (like WACCM-X) require time for the user-set, initial conditions of the modelled atmosphere to stabilize into a physical equilibrium. While other studies such as Solomon et al. (2018) allowed one year for minor chemical constituents to equilibrate, we found temperature and density appeared to equilibrate after one month. As a precaution, the first 4 months of each dataset were ignored, leaving 12 model months for each CO_2 concentration modelled. Along with the 10 simulations stated earlier, an additional 64 month simulation of the year 2000 has also been completed. 64 months was chosen as 12 months are simulated 5 times, with the end of one simulated year being used as the initial conditions of the next 12 month cycle. Again 4 months are added to the start of this for equilibration. Figure 3 plots the differences for each of 5 cycles from the overall globally averaged temperature and globally averaged density altitude profiles for the 64 month simulation of the year 2000 (with the first 4 months ignored).

3 Processing

A geopotential height, h, is output at each of the grid points of WACCM-X. This was converted into a geometric altitude, z, via

$$z = h\left(1 - \frac{h}{r_E}\right) \tag{1}$$

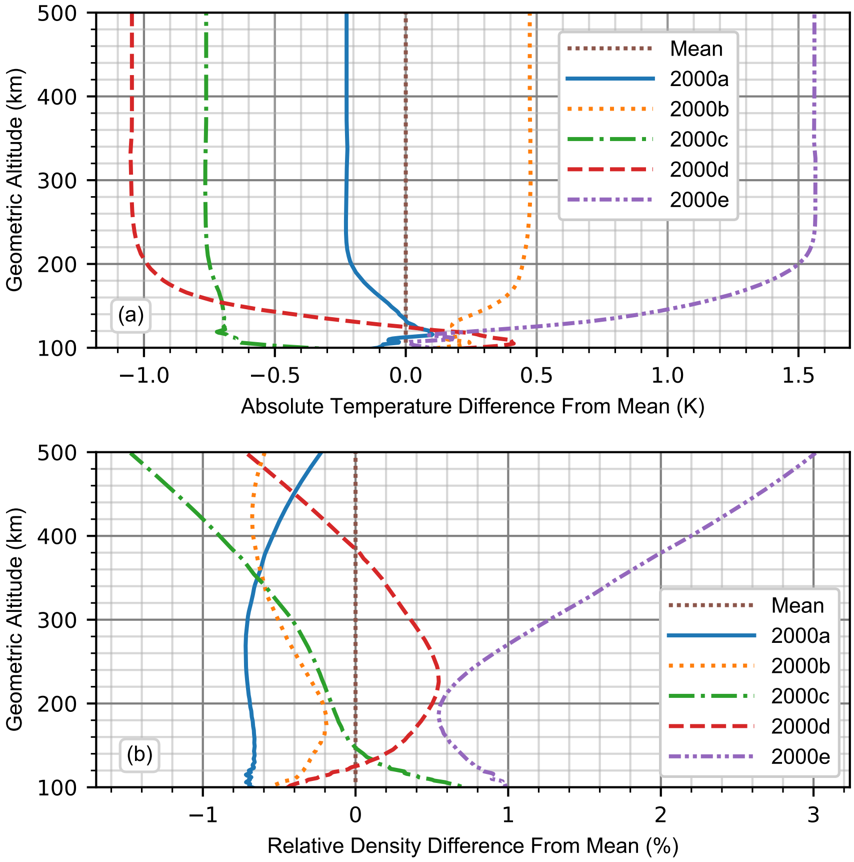

Figure 3. Interannual variability within WACCM-X when cyclically repeating the year 2000 under low solar activity ($F_{10.7}$=70 and Kp=0.33) and leaving all else as default. (a) The absolute difference in temperature of each annual mean from the overall 5 cycle mean (exospheric temperature of 589.3 K). (b) The relative difference in neutral density of each annual mean from the overall 5 cycle mean.

where r_E is the average radius of the Earth, 6371 km. The geometric altitude is equivalent to a satellite's orbiting altitude. All interpolation between points on this grid was performed via 1-D monotonic cubic interpolation.

WACCM-X models the thermosphere down to a pressure level of 4×10^{-10} hPa. This minimal pressure level varies in height, with the maximum altitude decreasing as the thermosphere cools. At high ground-level CO_2 concentrations the maximum model altitude is only 280 km. As the motivation of the work was to understand the reduction in density at commonly used LEO altitudes, the WACCM-X model data was extrapolated to an altitude of 500 km. It was found that the function that best fit the densities at points above 175 km for all cases was calculated by

$$\rho(z) = az^b log(z + c) + d \tag{2}$$

where ρ is atmospheric density and a, b, c and d are coefficients fit to the modelled density with non-linear least squares. This allowed a neutral density profile as a function of altitude to be obtained for each latitude-longitude combination. Temperatures in the thermosphere tend towards the exospheric temperature with increasing altitude. It is assumed the temperature at the highest modelled altitude is the exospheric temperature, and therefore this temperature is used for all higher altitudes up to 500 km.

To obtain global mean annual mean values of temperature and density, data was transformed from the model's pressure levels to geometric altitudes using the above methods, and then averaged temporally to calculate annual means at each altitude, latitude and longitude. The global mean annual mean is then obtained by averaging over latitude (with cosine latitude weighting) and longitude.

4 Results

Figure 4a and b show the WACCM-X global mean temperature plotted against ground-level CO_2 concentration at the fixed pressure level of 2.9×10^{-7} mbar (around 200 km altitude) during the March equinox and June solstice. This was done to compare the WACCM-X data at large CO_2 concentrations against three implementations of the Coupled Middle Atmosphere Thermosphere version 2 (CMAT2) model (Cnossen et al., 2009), where each implementation has different gravity wave parameterization schemes. While WACCM-X is cooler than all three implementations of the CMAT2 model, WACCM-X's temperature decreases with increasing CO_2 as expected, and at a similar rate to that of CMAT2.

Using the methods described in this study, the trend of decreasing neutral density due to increasing carbon dioxide for the period 1975-2005 has been calculated to be -5.8% per decade at 400 km altitude. This places it in the middle of the range predicted by other models and observations which were summarised in Table 1.

Stating trends for the reduction in neutral thermospheric density is useful for studies of historical periods, as the change in carbon dioxide concentration is fixed. However, for future reductions in density, CO_2 concentration will be variable and any future density trend will be dependent upon it. Figure 5 plots the relative reduction in density compared to the year 2000 against the ground-level CO_2 concentration.

Figure 6 shows the density change relative to the year 2000 for each RCP scenario. These data were generated by combining the data shown in Figures 1 and 5. Under the high emissions RCP8.5 scenario, the neutral density relative to the year 2000 reduced by 75% at 400 km by the year 2095. Under the RCP2.6 scenario, neutral densities at 400 km reach their largest change between the years 2040 and 2060 as CO_2 concentrations peak and begin to decline. This peak sees global ground-level temperature rise limited to 2 degrees or below and a 25% reduction in neutral density compared to the year 2000. Neutral densities recover to a 20% reduction by 2100. Regardless of scenario, the WACCM-

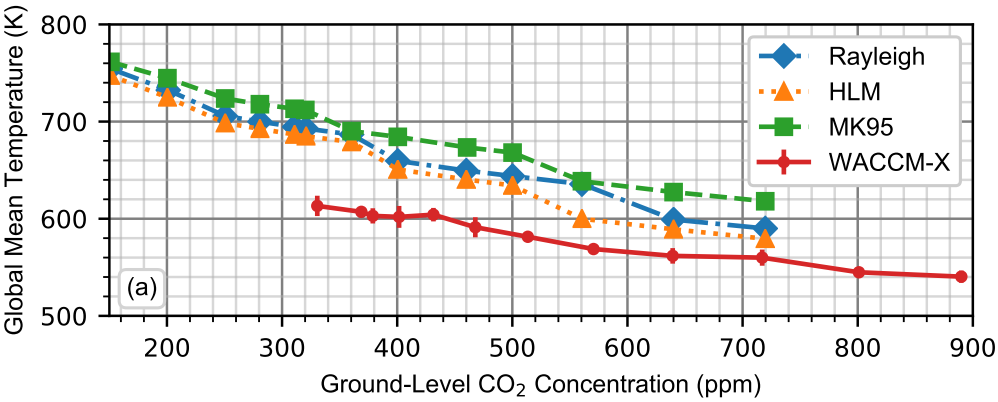

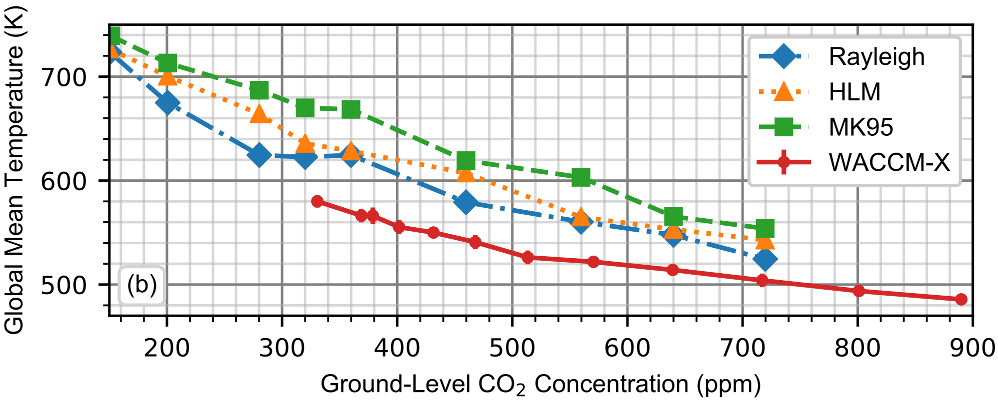

Figure 4. Global mean temperature against ground-level CO_2 concentration at a fixed pressure of 2.9×10^{-7} mbar (around 200 km altitude), with the Rayleigh, HLM and MK95 gravity wave implementations of CMAT2, as taken from Figure 5 of (Cnossen et al., 2009). These models were run with $F_{10.7} = 80$ and $Kp = 2$. WACCM-X was run at $F_{10.7} = 70$ and $Kp = 0.33$. (a) is for the March equinox (80th day of the year) while (b) is for the June solstice (172nd day of the year). WACCM-X global mean temperature means and errors are calculated from 21 days of data centred on the given dates.

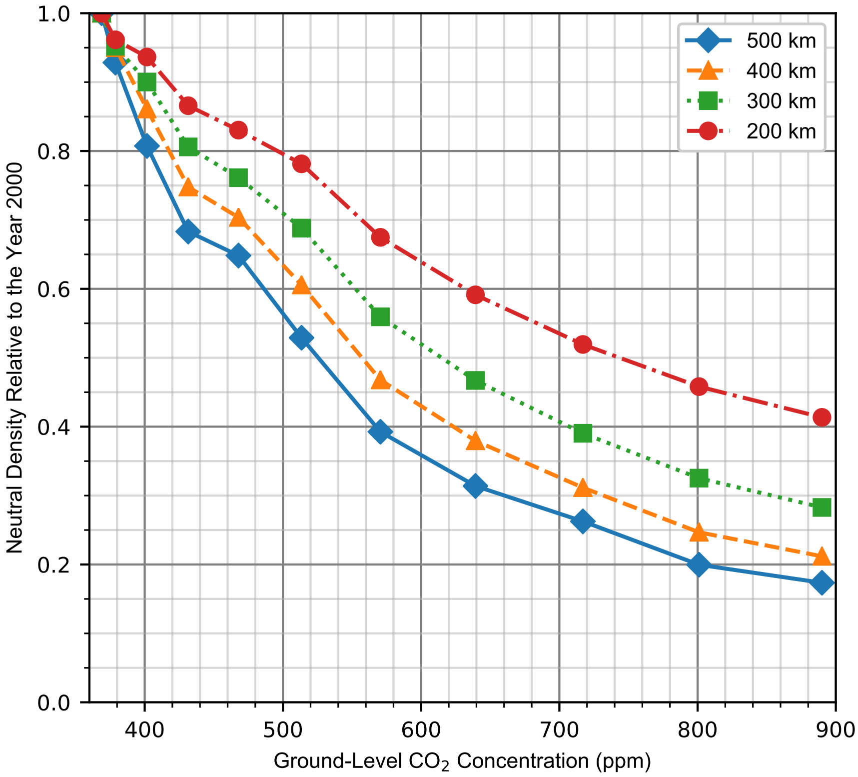

Figure 5. Reductions in neutral density relative to the year 2000 as the ground-level CO_2 concentration increases, for 200, 300, 400 and 500 km altitudes.

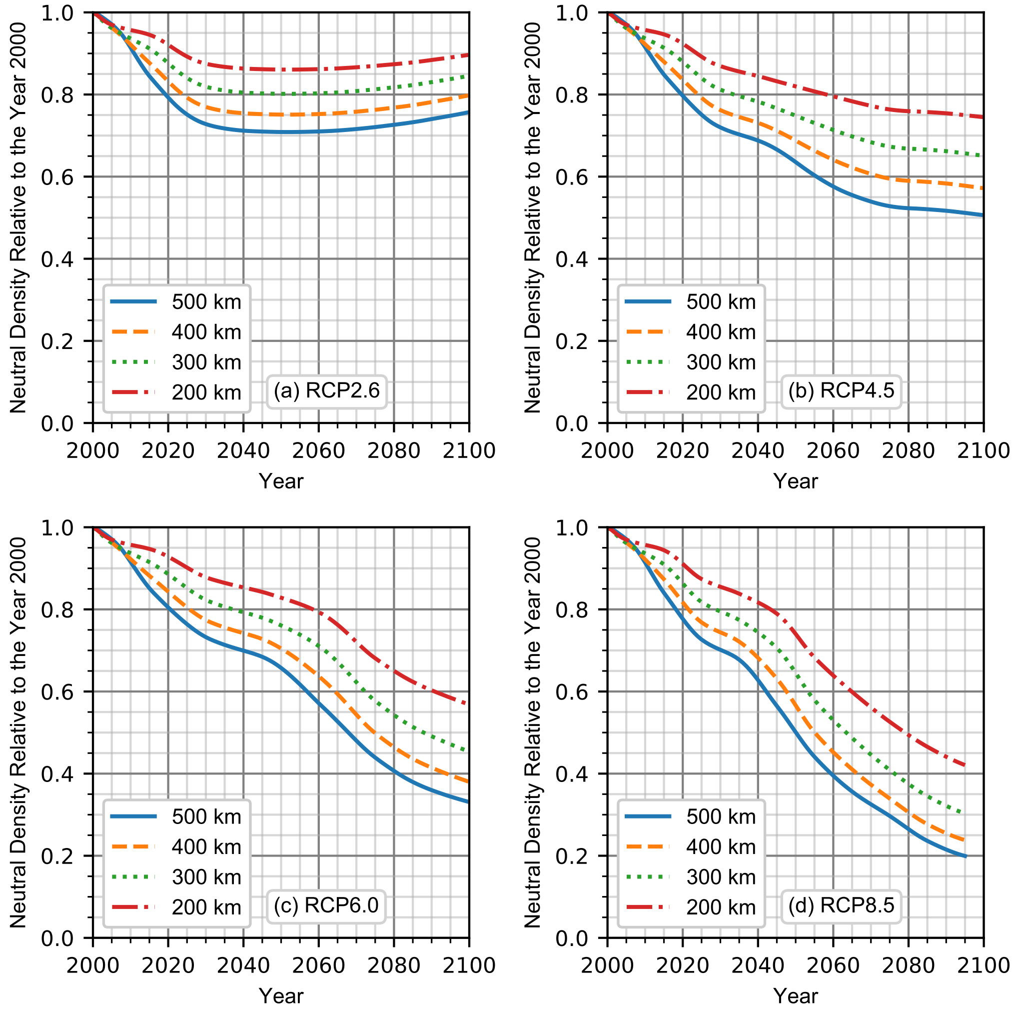

Figure 6. Global mean neutral density relative to the year 2000 over time for each of the IPCC RCP scenarios at the given altitudes. RCP8.5 (d) is truncated as no runs were performed for the largest CO_2 values.

X model shows that neutral densities have dropped by 17% at 400 km in 2020 relative to the year 2000.

5 Discussion

The targets and predictions set out within the Paris Agreement can provide some further context to this work's results. The Emissions Gap Report from the United Nations Environment Programme (2019) states that for a 50% probability of limiting global warming to 1.5°C, the carbon budget from 2018 onward is 580 $GtCO_2$. Taking the 2017 globally averaged CO_2 concentration of 405.0 ppm (Le Quéré et al., 2018), this sets a target of 480 ppm above which there is higher than 1.5°C warming at ground level. This target is independent of time and is reached in different years in the RCP scenarios. By looking at the density reductions in Figure 5, it can be seen that the 1.5 degree warming target is equivalent to a 30% drop in neutral density at 400 km relative to the year

Table 2. Orbital lifetimes of objects with the density reduction due to higher ground-level CO_2 concentrations applied. The lifetime ratio is the lifetime at the given CO_2 value relative to the lifetime during the year 2000. The initial state of each object was given by the two line element set on November 2nd 2020 with use of the North American Aerospace Defense (NORAD) satellite catalog number. Coefficient of drag for all objects was set as C_d=2.0.

Object	ISS	Starlink-60	MicroSat-R Debris	EQUISat
NORAD ID	25544	43510	44134	43552
Perigee / km	417	371	272	310
Apogee / km	420	373	845	312
Area / Mass Ratio (m^2kg^{-1})	0.0034	0.0176	0.0053	0.00077
Lifetime in year 2000 (379 ppm)	1618.9	84.6	959.4	76.7
Lifetime at 468 ppm	2131.4	112.2	1214.5	98.7
Lifetime ratio at 468 to 379 ppm	1.32	1.33	1.27	1.29
Lifetime at 890 ppm	4884.1	309.0	2599.5	248.6
Lifetime ratio at 890 to 379 ppm	3.02	3.65	2.71	3.24

2000. For a 66% probability of limiting warming to 1.5°C, there is a remaining budget from 2018 of 420 $GtCO_2$. This is equivalent to a concentration of 459 ppm and a drop of 27% in neutral density at 400 km. The Emissions Gap Report also gives a prediction that under the current unconditional Nationally Determined Contributions (NDCs) and assuming a linear trajectory through to 2030, cumulative emissions are predicted to be around 510 $GtCO_2$ until 2030. So under current circumstances, we are likely to see a CO_2 concentration of 470 ppm in the year 2030, which corresponds to a 28.5% drop in neutral density at 400 km between the year 2000 and 2030.

The empirical atmospheric model NRLMSISE-00 (Picone et al., 2002) is one of the thermospheric models used in space debris models and is calibrated with observational data up to the year 1997. The relative density drop seen in Figure 5 can therefore be used as a scaling factor for the neutral density output from NRLMSISE-00 to account for the density trends from increases in CO_2. This has been done for a few objects in LEO in Table 2. A simple numerical propagator was used, with drag as the only perturbing force and NRLMSISE-00 as the density model. The changes presented here are to provide initial implications of the work for the debris environment. The lifetimes at 468 ppm was chosen as the closest modelled point using WACCM-X to the 1.5 degree target CO_2 of 480 ppm. The orbital lifetimes of the chosen objects increase by between 27% and 33% relative to the year 2000. Under the highest modelled CO_2 concentration of 890 ppm, the orbital lifetime approximately triples when compared to the year 2000.

If these increases in orbital lifetime are experienced by all objects, they will have a substantial impact upon the space debris environment in at least two ways. Firstly the number of orbiting objects will increase. The number of objects can only increase by adding new objects (most commonly via launches), or having orbiting objects collide and create collision fragments. Longer lifetimes lead to a greater cumulative chance of collison, resulting in further fragmentation events. Secondly, operators who meet the 25 year guideline by using atmospheric drag to passively remove their satellite from orbit will have to take the reduction in density into account by lowering the perigee of their final orbit or by using a larger drag augmentation device. In both cases, further satellite mass has to be dedicated to the change.

These results have been computed under low solar activity only. Therefore it is only appropriate to apply these density reductions at solar minima. There will still be a secular density reduction when looking at solar maxima, albeit smaller (see Emmert (2015)). It is unknown to what scale this will be and this will be the subject of future work. The density reduction is expected to scale with the solar activity between the minima and maxima, albeit the exact relationship is unknown. It is acknowledged that a number of assumptions have had to be made to allow for the modelling of future densities. These include the value of k_q, extrapolation to higher altitudes and ignoring the density change due to the Earth's changing magnetic field. However, validation against previous studies by looking at historic trends and the impact on global mean temperatures under increasing CO_2 concentrations have shown the base of the model is within the bounds of currently published literature.

6 Conclusion

Increasing ground-level CO_2 concentrations result in decreasing thermospheric densities. These have been historically observed and modelled as summarized in Table 1. The impact on neutral densities under further increasing CO_2 concentrations have been modelled and presented within Figure 5. These neutral density reductions were also estimated for the four IPCC RCP scenarios in Figure 6. Density reductions reported throughout the paper have been given relative to the density in the year 2000 (under low solar activity) to provide a scaling ratio which can be applied to fast, empirical atmospheric models such as NRLMSISE-00. It has also been shown that limiting warming to the 1.5°C target of the Paris Agreement will still result in a 27-30% reduction in density relative to the year 2000 at 400 km, with orbital lifetimes increasing by around 30% as a result. Even under the low CO_2 emissions of the RCP2.6 scenario, the drop in neutral density will have a substantial impact on LEO object orbital lifetimes, as well as the debris environment within this region. Any CO_2 concentrations higher than this will have an even more substantial impact on thermospheric densities and the space industry as a whole, particularly on constellations relying on atmospheric drag to passively remove their satellites from orbit.

Acknowledgments

The authors acknowledge the contributions of those who helped develop CESM and WACCM-X. These models are publicly available from http://www.cesm.ucar.edu/models/.

The authors further acknowledge the use of the IRIDIS High Performance Computing Facility, and associated support services at the University of Southampton, in the completion of this work.

This work and M. K. Brown was supported by the Natural Environment Research Council (NERC) (NE/L002531/1). A. J. Kavanagh is supported by NERC (NE/R016038/1). I. Cnossen is supported by an Independent Research Fellowship from NERC (NE/R015651/1).

The data produced and processed for this study is available at doi:10.5285/0bb41477e0a5416190459433cb5ab907

References

Cnossen, I. (2014). The importance of geomagnetic field changes versus rising CO2 levels for long-term change in the upper atmosphere. *Journal of Space Weather and Space Climate*, *4*, 8. doi: 10.1051/swsc/2014016

Cnossen, I., Harris, M. J., Arnold, N. F., & Yiĝit, E. (2009). Modelled effect of changes in the CO2 concentration on the middle and upper atmosphere: Sensitivity to gravity wave parameterization. *Journal of Atmospheric and Solar-Terrestrial Physics*, *71*(13), 1484–1496. doi: 10.1016/j.jastp.2008.09.014

Cnossen, I., & Maute, A. (2020). Simulated Trends in Ionosphere-Thermosphere Climate Due to Predicted Main Magnetic Field Changes From 2015 to

2065. *Journal of Geophysical Research: Space Physics*, *125*(3), 1–11. doi: 10.1029/2019JA027738

Emmert, J. T. (2015). Altitude and solar activity dependence of 1967–2005 thermospheric density trends derived from orbital drag. *Journal of Geophysical Research: Space Physics*, 2940–2950. doi: 10.1002/2015JA021047.Received

Emmert, J. T., Drob, D. P., Shepherd, G. G., Hernandez, G., Jarvis, M. J., Meriwether, J. W., … Tepley, C. A. (2008). DWM07 global empirical model of upper thermospheric storm-induced disturbance winds. *Journal of Geophysical Research: Space Physics*, *113*(11), 1–16. doi: 10.1029/2008JA013541

ESA Space Debris Office. (2020). Annual Space Environment Report. (September).

Feofilov, A. G., Kutepov, A. A., She, C. Y., Smith, A. K., Pesnell, W. D., & Goldberg, R. A. (2012). CO2(v2)-O quenching rate coefficient derived from coincidental SABER/TIMED and Fort Collins lidar observations of the mesosphere and lower thermosphere. *Atmospheric Chemistry and Physics*, *12*(19), 9013–9023. doi: 10.5194/acp-12-9013-2012

Hathaway, D. H. (2015). The solar cycle. *Living Reviews in Solar Physics*, *12*(1). doi: 10.1007/lrsp-2015-4

IPCC. (2014). *Climate Change 2014 Synthesis Report.* doi: 10.1017/CBO9781107415324

Keating, G. M., Tolson, R. H., & Bradford, M. S. (2000). Evidence of long term global decline in the Earth's thermospheric densities apparently related to anthropogenic effects. *Geophysical Research Letters*, *27*(10), 1523–1526.

Laštovička, J., Akmaev, R. A., Beig, G., Bremer, J., & Emmert, J. T. (2006). Global Change in the Upper Atmosphere. *Science*, *314*(5803), 1253–1254. doi: 10.1126/science.1135134

Le Quéré, C., Andrew, R. M., Friedlingstein, P., Sitch, S., Pongratz, J., Manning, A. C., … Zhu, D. (2018). Global Carbon Budget 2018. *Earth System Science Data Discussions*, *pre print*(November), 1–54. Retrieved from `https://www.earth-syst-sci-data.net/10/2141/2018/essd-10-2141-2018.pdf` doi: 10.5194/essd-2017-123

Liu, H. L., Foster, B. T., Hagan, M. E., McInerney, J. M., Maute, A., Qian, L., … Oberheide, J. (2010). Thermosphere extension of the Whole Atmosphere Community Climate Model. *Journal of Geophysical Research: Space Physics*, *115*(12), 1–21. doi: 10.1029/2010JA015586

Mlynczak, M. G., Hunt, L. A., Russell, J. M., Marshall, B. T., Mertens, C. J., & Thompson, R. E. (2016). The global infrared energy budget of the thermosphere from 1947 to 2016 and implications for solar variability. *Geophysical Research Letters*, *43*(23), 11,934–11,940. doi: 10.1002/2016GL070965

Picone, J. M., Hedin, A. E., Drob, D. P., & Aikin, A. C. (2002). NRLMSISE-00 empirical model of the atmosphere: Statistical comparisons and scientific issues. *Journal of Geophysical Research: Space Physics*, *107*(A12), 1–16. doi: 10.1029/2002JA009430

Qian, L., Roble, R. G., Solomon, S. C., & Kane, T. J. (2006). Calculated and observed climate change in the thermosphere, and a prediction for solar cycle 24. *Geophysical Research Letters*, *33*(23), 1–5. doi: 10.1029/2006GL027185

RCP Database. (2009). *http://www.iiasa.ac.at/web-apps/tnt/RcpDb.*

Roble, R. G., & Dickinson, R. E. (1989). How will changes in carbon dioxide and methane modify the mean structure of the mesosphere and thermosphere? *Geophysical Research Letters*, *16*(12), 1441–1444. doi: 10.1029/GL016i012p01441

Saunders, A., Lewis, H. G., & Swinerd, G. G. (2011). Further evidence of long-term thermospheric density change using a new method of satellite ballistic coefficient estimation. *Journal of Geophysical Research: Space Physics*, *116*(10), 1–15. doi: 10.1029/2010JA016358

Sharma, R. D., & Roble, R. G. (2002). Cooling mechanisms of the planetary thermospheres: The key role of O atom vibrational excitation of CO2 and NO. *ChemPhysChem*, *3*(10), 841–843. doi: 10.1002/1439-7641(20021018)3:10⟨841::AID-CPHC841⟩3.0.CO;2-4

Solomon, S. C., Liu, H. L., & Marsh, D. R. (2019). Whole Atmosphere Climate Change : Dependence on Solar Activity. *Journal of Geophysical Research : Space Physics*, 3799–3809. doi: 10.1029/2019JA026678

Solomon, S. C., Liu, H. L., Marsh, D. R., McInerney, J. M., Qian, L., & Vitt, F. M. (2018). Whole atmosphere simulation of anthropogenic climate change. *Geophysical Research Letters*, *45*(3), 1567–1576. doi: 10.1002/2017GL076950

Solomon, S. C., Qian, L., & Roble, R. G. (2015). New 3-D simulations of climate change in the thermosphere. *Journal of Geophysical Research: Space Physics*, *120*(3), 2183–2193. doi: 10.1002/2014JA020886

Thébault, E., Finlay, C. C., & Beggan, C. D. (2015). International geomagnetic reference field: The 12th generation international geomagnetic reference field - The twelfth generation. *Earth, Planets and Space*, *67*(1). doi: 10.1186/s40623-015-0228-9

United Nations Environment Programme. (2019). *Emissions Gap Report 2019.*